

On wind resistant properties of Tiger Gate suspension bridge

H.F. Xiang[†], A.R. Chen[‡] and J.Z. Song[†]

Department of Bridge Engineering, Tongji University, Shanghai, 200092, China

Abstract. Tiger Gate Bridge, a steel suspension bridge with a main span of 888 m and a stiffening box girder, is located at the Pearl River Estuary, Guangdong Province, one of the typhoon-prone area in China. Focusing on the developing of the full aeroelastic model of the bridge and simulation of the wind field of the bridge site in a large boundary wind tunnel at Tongji University, Shanghai, China, some main results about the wind resistant properties of the bridge including aerodynamic instability, buffeting responses both being in operation and erection stages by using of a full aeroelastic model wind tunnel testing are introduced. Some of analytical approaches to those aerodynamic behaviours are also presented, and compared with experimental data of the testing.

Key words: suspension bridge; wind-resistant property; full aeroelastic model testing; flutter; buffeting.

1. Introduction

Tiger Gate Bridge, located at the Pearl River Estuary, Guangdong Province, one of the typhoon-prone area in China, is a steel box girder stiffened suspension bridge with a main span of 888 m, a deck of 35.6 m width and two pylons of 150 m height as shown in Fig. 1., which was opened to

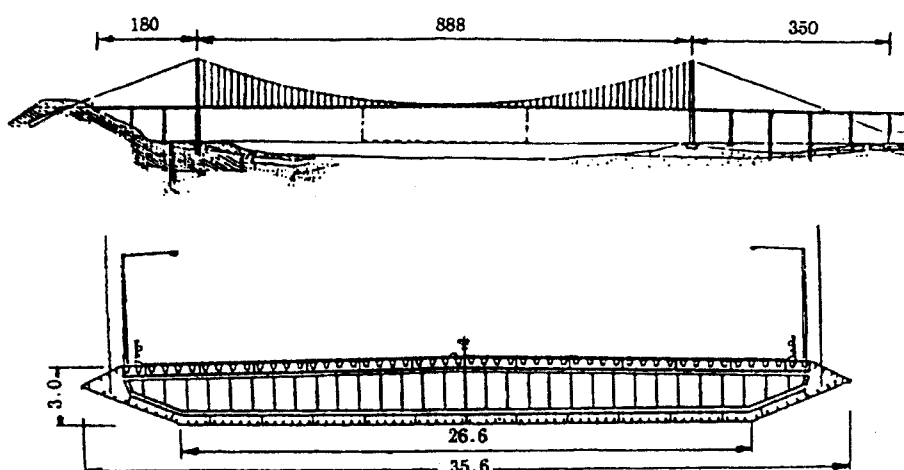


Fig. 1 General view of Tiger Gate Bridge(Unit: m)

[†] Professor

[‡] Associate Professor

traffic in 1997.

As the bridge site is often hit by typhoon 3 or 4 times a year, the wind resistant property of the bridge including the aerodynamic instability and buffeting response both being in operation and under construction stages were one of the main concerns at its design stage. To guarantee the safety of the bridge under action of strong wind, a sectional model and a full aeroelastic model with a geometrical reduced scale of 1/100 were conducted in TJ-1 and TJ-3 boundary layer wind tunnels at Tongji University respectively. The TJ-3 Boundary Wind Tunnel has a test section of 15 m wide, 2 m high and 14 m long with a wind speed range from 0 to 18 m/s. The testing was done for choice of a appropriate aerodynamic shapes of the stiffening girder and the bridge towers, identification of aerodynamic coefficients, checking of flutter instability and measuring of buffeting responses. This paper, focusing on the developing of the full aeroelastic model and simulation of the natural wind field in the TJ-3 Boundary Wind Tunnel, will mainly introduce the testing results and some of analytical approaches about the flutter instability and buffeting responses for the bridge both being in operation and under construction stages.

2. Aeroelastic full model of Tiger Gate Bridge

The skeleton of the model of the box stiffening girder was designed as a stainless steel box girder coated by a wooden cloth to simulate the stiffness and geometric shape respectively. Considering the testing for erection stages of the stiffening girder, during which the stiffening girder segments will be temporarily connected as rotational hinges, the stainless box girder skeleton is separated into segments of 24 cm and the segments are connected each other with two pieces of steel plates at both bottom and top of connection joints. The top ones can be moved away for the testing of erection stages of the girder for simulating the temporary hinge connection.

The model of the pylon is composed of a frame of steel skeleton with exterior Plexiglas forms by which the geometric shape of the actual structure was simulated. The wind tunnel testing for free standing stage of the tower has also been done.

The model of the cable is composed of a steel string wire and additional weight pieces made of copper bar. The steel wire was used to simulate the axial stiffness and the cylindrical weight pieces were placed at certain interval to simulate mass and drag force considering the effect of Reynolds Number as the model for the Akashi Kaikyo Bridge (Miyata 1995). Actually we did

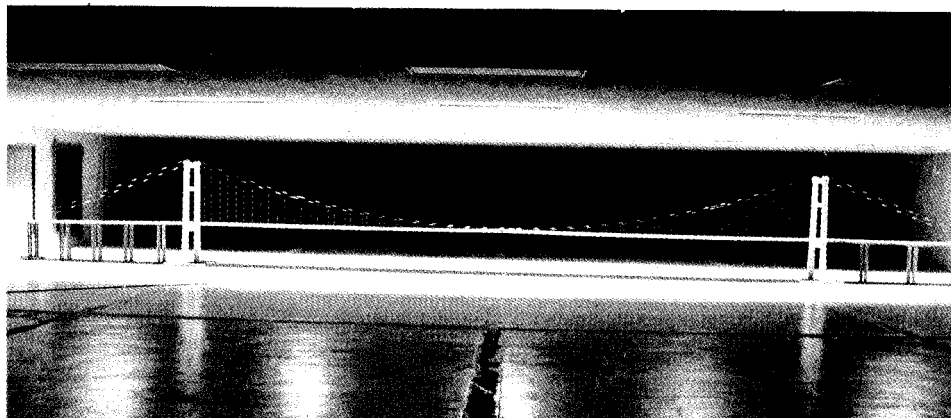


Fig. 2 Full aeroelastic model of Tiger Gate Bridge in TJ-3 boundary wind tunnel at Tongji University

Table 1 Structural properties of the full bridge model

Mode	Frequency of real bridge(Hz)	Frequency of model(Hz)		Measured damping ratio
		Required	Measured	Full model
1st. symm. transverse bending	0.0882	0.882	0.832	0.024
2nd. anti-symm. transverse bending	0.2809	2.809	2.639	0.027
1st. symm. torsion	0.3612	3.612	3.641	0.009
2nd. symm. torsion	0.4260	4.260	4.253	0.01
1st. symm. vertical bending	0.1715	1.715	1.690	0.007
2nd. symm. vertical bending	0.2251	2.251	2.354	0.007
3rd. symm. vertical bending	0.3682	3.682	3.550	0.007
4th. symm. vertical bending	0.5825	5.825	5.525	0.008
1st. anti-symm. vertical bending	0.1117(0.1587)	1.117	1.328	0.016
2nd. anti-symm. vertical bending	0.2765	2.765	2.658	0.004
3rd. anti-symm. vertical bending	0.4673	4.673	4.438	0.04

two sets of cable models, another with uniform weight pieces without considering the effect of the Reynolds Number but exact geometric shape of main cables.

Fig. 2 shows the completed full model in TJ-3 Wind Tunnel. Table 1 shows the dynamic properties of the model. The agreement between required frequencies and measured ones is good except the first antisymmetric vertical bending with longitudinal floating frequency. This is probably due to the friction existing between bearings at two ends of the model. The transverse mode damping is relatively higher, but others are small enough.

3. Simulation of turbulent wind field

A turbulent wind field was simulated in TJ-3 Boundary Layer Wind Tunnel by using spires and roughness blocks. Based on the measurement of wind characteristics at the bridge site and codes in Chinese "Wind Resistance Design Guideline for Highway Bridges" by Xiang, Lin and Chen (1996), the similarity of wind speed profile and wind spectrum as well as turbulence intensity at low speed was simulated, which are shown in Fig. 3 and Fig. 4.

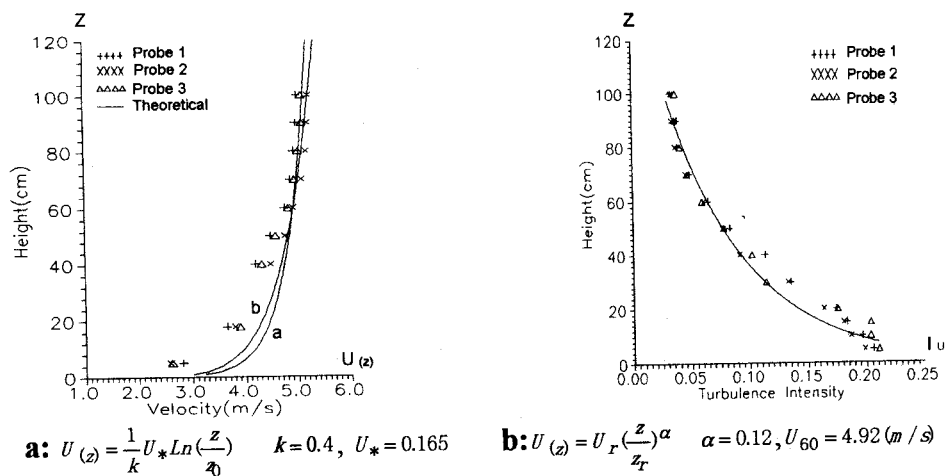


Fig. 3 Wind speed profile and distribution of turbulence intensity along height

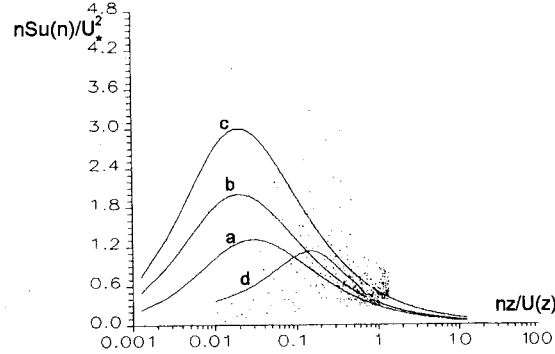


Fig. 4 Simulation of spectrum (a : Kaimal' Spectrum : $\frac{n S_u(n)}{u_*^2 \phi^{2/3}} = \frac{200 f}{(1 + 50 f)^{5/3}}$, $f = \frac{nz}{U(z)}$

b, c : Spectrum measured at the bridge site : $\frac{n S_u(n)}{u_*^2 \phi^{2/3}} = \frac{460 f}{(1 + 75 f)^{5/3}}$, $\phi^{2/3} = 1.0 \sim 1.5$

d : Spectrum simulated in wind tunnel, $U(z) = 4.19 \text{ m/s}$, $z = 0.65 \text{ m}$, $I_u = 6.2\%$

Fig. 3 shows the wind profile and the distribution of the turbulence intensity along height at a certain wind speed, which are also measured at different wind speed. As the boundary layer forming and stabilizing section is long enough and because of the use of passive turbulent generation instruments as spires and roughness blocks, both wind speed and turbulence intensity profiles keep same at different wind speeds.

From Fig. 4 it can be seen that the agreement between the simulated spectrum and the measured spectrum at the bridge site as well as the target spectrum (Kaimal' spectrum) is not good in the low frequency range, but it seems satisfactory at the frequency range of 1~6 Hz, in non-dimensional unit $nz/U(z)$, 0.2~1.0, which falls into the required frequency range of the model.

4. Flutter instability of Tiger Gate Bridge in operation

According to the Chinese "Wind Resistance Design Guideline for Highway Bridges" by Xiang, Lin and Chen (1996), the flutter critical wind speed of the bridge in uniform flow should satisfy the criterion :

$$U_{cr} \geq [U_{cr}] = 1.2 \mu_f U_d = 72 \text{ m/s} ; \text{ in range of } -3^\circ \leq \alpha \leq +3^\circ \quad (1)$$

in which $U_d = 50 \text{ m/s}$, is the bridge design standard wind speed at the deck level. α is the attack angle of air flow. The coefficient 1.2 is a principal safety factor including social importance of the structure, a destructive feature of flutter instability, reliability of experiment tests, design and construction of the bridge. The coefficient $\mu_f = 1.206$ is a conditional safety factor considering spatial effect of wind speed fluctuation (Xiang, Chen and Lin 1997). For the testing in the simulated turbulent flow, the factor $\mu_f = 1.0$ and the critical wind speed should be larger than 60 m/s.

Fig. 5 and Fig. 6 respectively show the evolution of total damping ratios including both structural and aerodynamic damping and the change of frequencies of the full model in uniform flow at 0° degree attack angle. Damping ratios for vertical bending modes increase quickly and the torsional frequency decreases as wind speed becomes higher.

The torsional displacement response at mid-span of the model under 0° degree attack angle is shown in Fig. 7. The wind speeds of 8.8 m/s (88 m/s for prototype) and 7.2 m/s (72 m/s for pro-

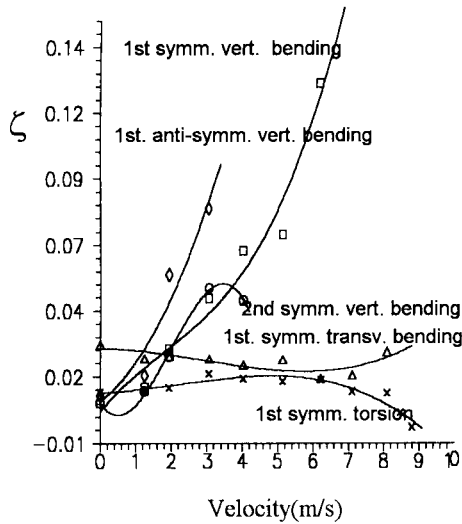


Fig. 5 Evolution of damping ratios

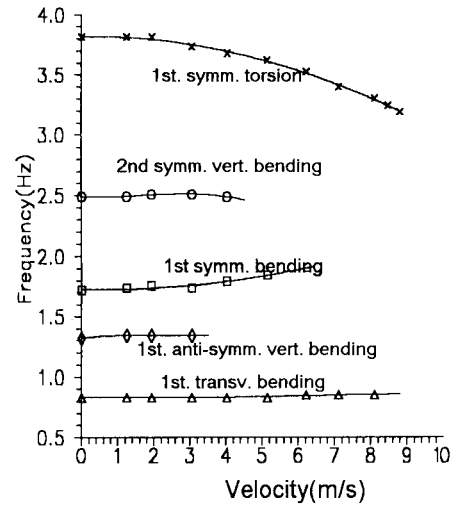


Fig. 6 Change of frequencies

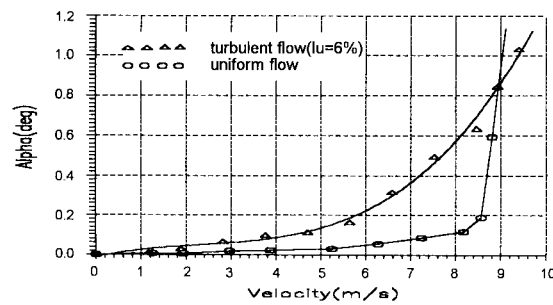


Fig. 7 Torsional angle(RMS) at mid-span under 0° degree attack angle

Table 2 Comparison between experimental results and analysis

	Attack angle of wind	
	+3°	0°
Spring-mounted sectional model testing	79	89
Full aeroelastic model testing	72	88
3-D finite element flutter analysis	78	88

tototype) are flutter onset wind speeds in uniform flow at 0° and $\pm 3^\circ$ degree attack angles respectively, while wind speed of 6.5 m/s (65 m/s for prototype) is the flutter onset speed in turbulent flow when RMS values of torsional displacements reach to 0.5°.

A 3-dimensional finite element model for flutter analysis was also developed and critical flutter wind speeds for the bridge both being in operation and under different erection stages of the stiffening girder were calculated by using a 3-D Finite Element Flutter Analysis Program, in which all the vibration modes are automatically searched to find a real flutter mode and all the aerodynamic coefficients including aerodynamic derivatives are directly adapted from sectional model testing in uniform flows. In all calculation the damping ratios for every modes are assumed to be 0.5%.

Table 2 shows the flutter onset wind speeds for the bridge in operation tested from spring mounted sectional model testings, full aeroelastic model testings in uniform flow and calculated

through 3-D finite element flutter analysis mentioned above. The agreement between experimental and analytical results is fairly good. Again the agreement between testings and analysis was also found for the flutter critical onset wind speed analysis of the bridge under different erection stages.

5. Flutter instability of Tiger Gate Bridge during erection

The stiffening girder of Tiger Gate Bridge was erected from mid-span extended to two sides. To avoid hitting of typhoon during the weakest construction stages, careful researches for wind resistance behaviors of the bridge during construction has been done through wind tunnel test and analysis.

The allowable design wind speed against flutter instability for the Tiger Gate Bridge under construction is 60 m/s, 0.84 of that in operation, with 10 years return period.

The evolution of the first symmetric vertical and torsional frequencies is shown in Fig. 8. The torsional frequency increases with increase of the length of erected girder, on the other hand, the vertical frequency keeps almost same.

The measured and analytical critical flutter wind speed under different erection stages is shown in Fig. 9, in which it should be noted that the critical wind speed for the erection stage 100% is just corresponding to the closure stage of the stiffening girder, at this moment there are no any second period dead loads for example the pavement. When the erection length reaches to 40% of the main span, the critical wind speed is about 75 m/s and when the erection length is less than 30% the main span, the critical wind speed does not meet the requirement. So, It was suggested that the stiffening girder should be erected to 40% of the main span before typhoon season comes.

Fig. 10 shows the RMS values of torsional displacements of the deck measured from the testing. The critical wind speeds at different erection stages were so determined that when the RMS values of torsional displacements of the deck reached to 0.5 degrees. From Fig. 10, we can see that, according to the criterion mentioned about, the existence of turbulence will shift the flutter to an earlier date compared with the model in uniform flows.

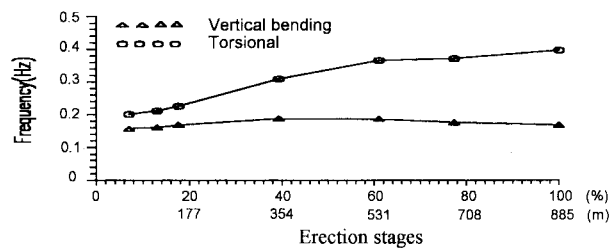


Fig. 8 Natural frequency under different erection stages

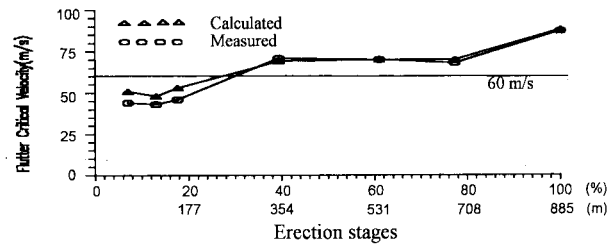


Fig. 9 Flutter critical wind speed under different erection stages

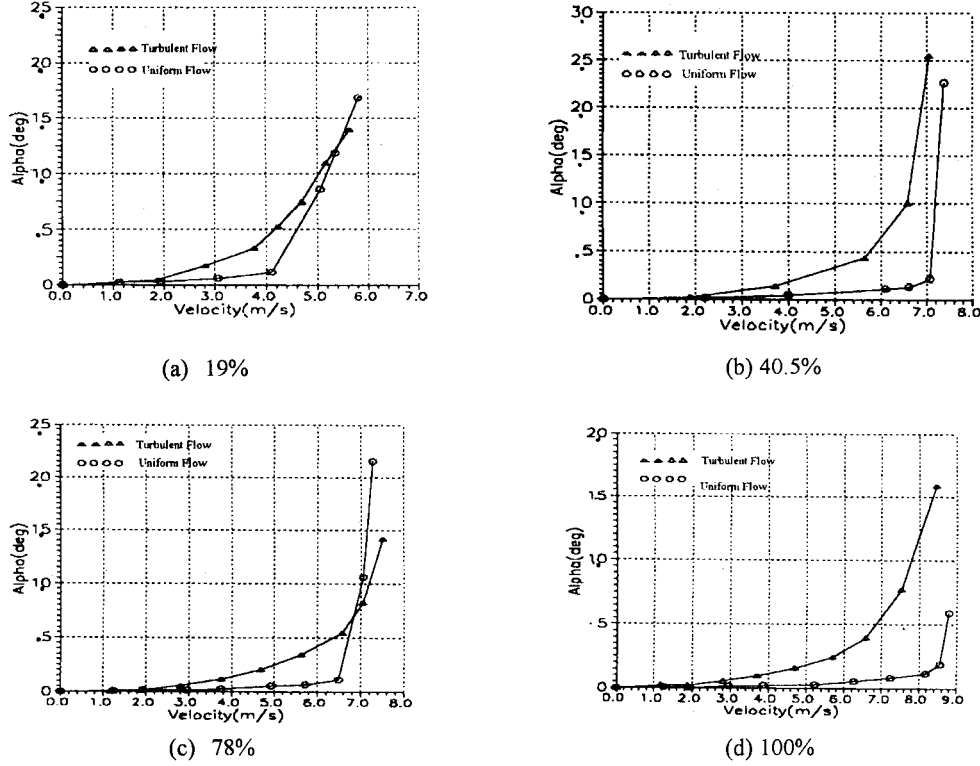


Fig. 10 RMS values of torsional displacements under different erection stages

6. Buffeting response of the Tiger Gate Bridge

The buffeting response of the Tiger Gate Bridge was obtained by using the frequency domain analysis method developed by Professor R.H. Scanlan and also the time domain analysis method, which was checked by full model wind tunnel in the simulated turbulent wind field.

Based on Scanlan's Buffeting Theory, in frequency domain, if the background responses are neglected, the vertical, torsional and transverse buffeting displacement response RMS (root-mean-square) values can be expressed as :

$$R_h(\omega_h) = \rho UB \frac{|q(x)|_{\max}}{\omega_h^2} \sqrt{\frac{\pi \omega_h}{4 \tilde{\zeta}_h} |J_h(\omega_h)|^2 S_L(\omega_h)} \quad (2)$$

$$R_\alpha(\omega_\alpha) = \frac{1}{2} \rho UB^2 \frac{|r(x)|_{\max}}{\omega_\alpha^2} \sqrt{\frac{\pi \omega_\alpha}{4 \tilde{\zeta}_\alpha} |J_\alpha(\omega_\alpha)|^2 S_M(\omega_\alpha)} \quad (3)$$

$$R_p(\omega_p) = \rho UB \frac{|s(x)|_{\max}}{\omega_p^2} \sqrt{\frac{\pi \omega_p}{4 \tilde{\zeta}_p} |J_p(\omega_p)|^2 S_D(\omega_p)} \quad (4)$$

in which ρ is the density of air; U is wind speed; B is width of the bridge deck; $q(x)$, $r(x)$, $s(x)$

Table 3 Wind-induced moment at mid-span

	Moment(kN-m)	
	Lateral	Vertical
Buffeting response RMS value	60865	5658
Buffeting response peak value	243462	22632
Static wind response	255210	35
Gust response factor	1.95	647
Seismic force	63100	7700

are respectively vertical, torsional and transverse vibration mode functions; ω_h , $\tilde{\omega}_\alpha$, ω_p are respectively vertical, torsional and transverse circular frequencies including aerodynamic stiffness effects; $\tilde{\zeta}_h$, $\tilde{\zeta}_\alpha$, $\tilde{\zeta}_p$, are respectively total damping ratios; $|J_n(\omega_h)|^2$ ($n=h, \alpha, p$) is the joint accept function, which reflects the spatial correlation characters of turbulent wind field; and $S_L(\omega_h)$, $S_M(\tilde{\omega}_\alpha)$, $S_D(\omega_p)$ are respectively vertical, torsional and transverse buffeting force spectra. For Tiger Gate Bridge, the Kaimal' and Panofsky-McCormick' Spectra are adapted and the Liepmann's formula was also used as the aerodynamic admittance function.

Table 3 shows the calculated internal forces at mid-span cross section due to static wind load and buffeting-induced dynamic load, in which the peak factor $g=4$ and the standard design wind speed $U_d=50$ m/s. The internal force due to seismic load with 3% of exceedance probability with a 100 years return period is also given for comparison, which shows that the wind-induced effect in main girder of the bridge is much larger than the seismic effect.

7. Concluding remarks

After the investigation of wind-resistant performance of Tiger Gate Bridge both being in operation and under construction stages, some results may be summarized as follows :

1. The effect of turbulence on flutter is significant for the bridge under different erection stages. For Tiger Gate Bridge, it was found that the critical flutter onset wind speed in turbulent flow is lower than that in uniform flow, if the the critical onset wind speed is so determined that when the RMS value of torsional displacements reaches to 0.5 degree. In turbulent wind field, for the bridge under different erection stages, sometimes significant flutter phenomena was observed and sometimes not.

2. The comparison was made between the experimental and analytical results, the agreement of flutter onset wind speed is fairly good not only for the bridge being in operation but also under different erection stages of the stiffening girder.

3. At earlier erection stages of the stiffening girder, because the torsional stiffness is relatively low, the flutter instability will not meet the requirement of the design criterion. The torsional frequency increases with the process of erection and the vertical frequency keeps almost constant. It was suggested that for Tiger Gate Bridge, the main girder should be erected to 40% of the total length before typhoon season comes.

References

- Miyata T. (1995), "Full model testing of large cable-supported bridges", A State of the Art in Wind Engineering, *Ninth International Conference on Wind Engineering*, New Delhi.
- Xiang. H. F, Lin, Z. X and Chen, A. R (1996) *Wind Resistance Design Guideline for Highway Bridges*,

People's Communication Press House of China.

- Xiang H. F. (1995) "Buffeting response analysis and control of long-span bridges", A State of the Art in Wind Engineering, *Ninth International Conference on Wind Engineering, New Delhi*.
- Xiang, H. F., Chen, A. R. and Lin, Z. X. (1997), "An introduction to the Chinese Wind Resistant Design Guideline of Highway Bridges", *Proceeding of 2nd European and African Conference on Wind Engineering*, Genova, Italy, June.